

UCLA

UCLA Previously Published Works

Title

Microbial and Metabolite Signatures of Stress Reactivity in Ulcerative Colitis Patients in Clinical Remission Predict Clinical Flare Risk.

Permalink

<https://escholarship.org/uc/item/3vn5h3b0>

Journal

Inflammatory Bowel Diseases, 30(3)

Authors

Jacobs, Jonathan

Sauk, Jenny

Ahdoot, Aaron

et al.

Publication Date

2024-03-01

DOI

10.1093/ibd/izad185

Peer reviewed

Microbial and Metabolite Signatures of Stress Reactivity in Ulcerative Colitis Patients in Clinical Remission Predict Clinical Flare Risk

Jonathan P. Jacobs, MD, PhD,^{*,†,‡,||} Jenny S. Sauk, MD,^{*,†,‡} Aaron I. Ahdoon, BS,[†] Fengting Liang, BS,[†] William Katzka, BA,[†] Hyo Jin Ryu, BS,[§] Ariela Khandadash, MBA,^{*} Venu Lagishetty, PhD,[†] Jennifer S. Labus, PhD,^{*,†,‡} Bruce D. Naliboff, PhD,^{*,‡} and Emeran A. Mayer, MD^{*,†,‡}

From the *G. Oppenheimer Center for Neurobiology of Stress and Resilience, University of California Los Angeles, Los Angeles, CA, USA

[†]Vatche and Tamar Manoukian Division of Digestive Diseases, Department of Medicine, David Geffen School of Medicine at UCLA, Los Angeles, CA, USA

[‡]Goodman-Luskin Microbiome Center, University of California Los Angeles, Los Angeles, CA, USA

[§]A.T. Still University School of Osteopathic Medicine in Arizona, Mesa, AZ, USA

^{||}Division of Gastroenterology, Hepatology and Parenteral Nutrition, Veterans Affairs Greater Los Angeles Healthcare System, Los Angeles, CA, USA

Address correspondence to: Jonathan P. Jacobs, MD, PhD, CHS A3-115, 10833 Le Conte Avenue, Los Angeles, CA, USA, (310) 825-9333, (JJacobs@mednet.ucla.edu).

Background: Stress reactivity (SR) is associated with increased risk of flares in ulcerative colitis (UC) patients. Because both preclinical and clinical data support that stress can influence gut microbiome composition and function, we investigated whether microbiome profiles of SR exist in UC.

Methods: Ninety-one UC subjects in clinical and biochemical remission were classified into high and low SR groups by questionnaires. Baseline and longitudinal characterization of the intestinal microbiome was performed by 16S rRNA gene sequencing and fecal and plasma global untargeted metabolomics. Microbe, fecal metabolite, and plasma metabolite abundances were analyzed separately to create random forest classifiers for high SR and biomarker-derived SR scores.

Results: High SR reactivity was characterized by altered abundance of fecal microbes, primarily in the Ruminococcaceae and Lachnospiraceae families; fecal metabolites including reduced levels of monoacylglycerols (endocannabinoid-related) and bile acids; and plasma metabolites including increased 4-ethyl phenyl sulfate, 1-arachidonoylglycerol (endocannabinoid), and sphingomyelin. Classifiers generated from baseline microbe, fecal metabolite, and plasma metabolite abundance distinguished high vs low SR with area under the receiver operating characteristic curve of 0.81, 0.83, and 0.91, respectively. Stress reactivity scores derived from these classifiers were significantly associated with flare risk during 6 to 24 months of follow-up, with odds ratios of 3.8, 4.1, and 4.9. Clinical flare and intestinal inflammation did not alter fecal microbial abundances but attenuated fecal and plasma metabolite differences between high and low SR.

Conclusions: High SR in UC is characterized by microbial signatures that predict clinical flare risk, suggesting that the microbiome may contribute to stress-induced UC flares.

Key Words: stress reactivity, flare prediction, microbiome, metabolomics, biomarkers

Introduction

Ulcerative colitis (UC) is a chronic inflammatory disorder of the colon which typically shows a relapsing-remitting course. The factors precipitating disease flare are not well understood, but patients frequently report stressful events as triggers and that effectively coping with stress improves their disease course.¹ This has been supported by multiple studies of UC demonstrating that high perceived stress is associated with increased risk of clinical flare.^{2–5} The key effectors of stress responses are the sympathetic branch of the autonomic nervous system (ANS) and the hypothalamic-pituitary-adrenal (HPA) axis. In a prospective study of UC patients in clinical remission, we identified a subset of patients

with increased stress perception based upon psychological instruments, which was characterized by higher sympathetic arousal on ANS testing but no difference in cortisol values.⁵ This profile was suggestive of a stress reactivity (SR) phenotype mediated by the sympathetic nervous system. Patients in the high SR group showed 3.6-fold increased risk of clinical flare during longitudinal follow-up.

These findings are consistent with animal models that have demonstrated that experimental stressors can exacerbate colitis.⁶ Acute and chronic stress have diverse effects on the gastrointestinal tract including altered regional gastrointestinal motility, immune function, intestinal blood flow, quality of mucus layer, and intestinal barrier function.^{7,8} Stress also modulates the gut microbiome, the complex microbial

Key Messages**What is already known?**

Ulcerative colitis patients frequently experience stress as a contributing factor to their disease course, and stress reactivity defined by psychological questionnaires is associated with clinical flares.

What is new here?

Ulcerative colitis patients with high stress reactivity can be distinguished from less stress-reactive UC patients by intestinal microbe, fecal metabolite, and plasma metabolite profiles, all of which are predictive of clinical flare risk.

How can this study help patient care?

Biomarkers of stress reactivity could identify UC patients at greatest risk of clinical flares who may benefit from stress-directed interventions and reveal stress-related microbiome-gut-brain pathways that may become future therapeutic targets.

communities inhabiting the digestive tract, which have a critical role in UC pathophysiology by influencing immune regulation and intestinal homeostasis.⁹ The effects of stress on the microbiome include altering gut microbial composition and function secondary to changes in regional gastrointestinal transit, promoting microbial virulence through binding of norepinephrine to microbial adrenergic-like receptors, and increasing access of gut microbes and their products to cells of the mucosal immune system due to impaired barrier function.¹⁰ Stress-induced mediators may also influence efferent and afferent pathways connecting the gut microbiome to the brain that have been implicated in affective disorders and gastrointestinal symptom generation.¹¹ In a model of despair behavior induced by chronic stress, administration of bacteria that had been depleted after chronic stress was sufficient to ameliorate stress-induced behavioral and metabolic phenotypes.¹²

We hypothesized that stress-induced changes in the gut microbiome contribute to the relationship of SR with clinical flare risk. To investigate this question in a human cohort, we assessed gut microbiome composition by 16S rRNA gene sequencing and function by fecal and plasma metabolomics. Ulcerative colitis patients in clinical remission with high SR demonstrated gut microbiome and fecal and plasma metabolite signatures that accurately differentiated them from the low SR group. Microbial and metabolite biomarkers of SR were also strongly predictive of clinical flare risk.

Methods**Participants**

This study included 91 subjects drawn from our previously described cohort of 110 biopsy-confirmed UC subjects between 18 and 65 years of age who were recruited from the UCLA Center for Inflammatory Bowel Diseases from June 20, 2018, to July 6, 2020.⁵ Subjects from the prior cohort who were in clinical and biochemical remission as defined by Simple Colitis Clinical Activity Index score (SCCAI) <5 and fecal calprotectin <150 µg/g were included in this analysis.¹³ Exclusion criteria included severe psychiatric disorders

as determined by the Mini International Neuropsychiatric Interview, use of 20 mg of prednisone or a higher dose, any changes in medication within 1 month prior to screening, use of antibiotics within 1 month of screening, and pregnancy or intention to become pregnant. All study procedures complied with the principles of the Declaration of Helsinki and were approved by the UCLA Institutional Review Board. All participants provided written informed consent prior to enrollment in the study.

Clinical Activity and SR Assessments

Subjects underwent initial screening at the time of a clinically indicated visit to the UCLA IBD clinic to confirm study eligibility based on SCCAI <5 and patient history. During the subject's next scheduled visit (baseline), the subject was asked to bring in fresh frozen stool obtained the morning of the visit and provide blood samples. Subjects then completed psychological and clinical assessments. In our prior study, high and low stress groups were based upon 4 parameters: Perceived Stress Scale (PSS), International Personality Item Pool—Neuroticism (IPIP-N), Hospital Anxiety and Depression Scale—Anxiety (HADS-A), and Hospital Anxiety and Depression Scale—Depression (HADS-D).⁵ As HADS-A and HADS-D measure psychological comorbidity, here SR groups were defined by only PSS (perceived ongoing stress) and IPIP-N (emotional reactivity to stressors).

The primary measure of disease activity during 1 to 2 years of longitudinal follow-up was the SCCAI, which has been validated for both physician ratings and patient self-report.^{13,14} Subjects completed a web-based questionnaire for self-reported SCCAI every 2 weeks during the longitudinal phase of the study. Clinical flares were defined as SCCAI ≥5.⁵ If participants reported SCCAI consistent with a clinical flare, they were contacted to schedule a study visit for blood and fecal sample collection. This was only performed for the first clinical flare. Quarterly visits (ie, every 3 months) were scheduled for clinical assessment and blood and fecal sample collection through the 1 to 2-year monitoring period. Study visits occurred from June 26, 2018, to June 23, 2021.

Fecal Sample Collection and Calprotectin Measurement

Fecal samples were collected at baseline, every 3 month during quarterly visits, and at the time of clinical flare. Participants were provided with home stool collection kits and asked to collect 2 sample types: preserved stool fixed in 95% ethanol and fresh frozen stool that was immediately placed in their home freezer after collection or in an insulated container with U-tek freezer packs that were precooled to approximately -20°C in their home freezers. Frozen samples were brought to study visits within 24 to 48 hours of collection. Study coordinators then transferred samples to lab freezers for long-term storage at -80°C. Frozen fecal samples were later ground into a coarse powder by mortar and pestle under liquid nitrogen, then aliquoted. Aliquots of frozen stool collected at baseline (all subjects), quarterly visits (subjects who later experienced clinical flare), and at the time of flare underwent fecal calprotectin measurement by ELISA according to the manufacturer's instructions (Eagle Biosciences, Inc.).

Fecal 16S rRNA Gene Sequencing

DNA extraction by bead beating and amplification of the V4 hypervariable region of the 16S rRNA gene were performed

according to our published protocol.^{15,16} Sequencing libraries underwent 2×250 sequencing using an Illumina NovaSeq 6000 SP flow cell (baseline samples from 90 subjects) or Illumina MiSeq v2 kit (longitudinal samples from 27 subjects who experienced a clinical flare) to a mean depth of 279,311 (range 125,670–870,299) and 40,597 (range 19,628–61,613) merged sequences per sample, respectively. Samples in each of the 2 sequencing runs were separately processed using the DADA2 R package to generate tables of denoised amplicon sequence variants (ASVs) for cross-sectional and longitudinal analyses.¹⁷ Taxonomy was assigned to ASVs using the SILVA 138.1 database.

Fecal and Plasma Metabolomics

Frozen aliquots of fecal samples and plasma collected at baseline ($n = 90$ and $n = 88$, respectively) and at the time of clinical flare ($n = 30$ and $n = 22$, respectively) were shipped to Metabolon, Inc., for analysis on their global HD4 metabolomics platform as a single batch. Original scale data from Metabolon were processed as previously described.¹⁸ In brief, metabolites that were detected in over 30% of samples were retained, and missing data were imputed using k-nearest neighbors. Metabolomics data subsequently underwent log₂ transformation and normalization by the vsn2 package in R prior to downstream analyses. Pathway assignments were provided by Metabolon for each metabolite.

Alpha and Beta Diversity Analyses

Alpha diversity analysis was performed for each 16S data set rarefied to the lowest sequence depth sample using the Shannon index of richness and evenness calculated with the phyloseq package in R.¹⁹ Significance was assessed by multivariate ANOVA (cross-sectional analysis) using the aov function in R or by a linear mixed-effects model (longitudinal analysis) using the lme4 R package with subject as a random effect; sex, age, and body mass index (BMI) were covariates in both models. Beta diversity analysis using Bray-Curtis dissimilarity was performed for 16S rRNA gene sequencing data after filtering to retain ASVs present in at least 10% of samples then visualized by principal coordinates analysis (PCoA). Fecal and plasma metabolomics data were analyzed using Euclidean distance and visualized by PCoA. The significance of differences in Bray-Curtis dissimilarity or Euclidean distance was assessed using permutational multivariate analysis of variance (PERMANOVA) implemented with the adonis2 function of vegan with 10 000 permutations.²⁰ Adonis2 was run by “margin,” which calculates the marginal R^2 for each variable after adjusting for age, sex, and BMI. For longitudinal analyses, subject was used as strata for permutation.

Differential Abundance Testing

Differentially abundant microbes were identified using multivariate general linear models implemented in MaAsLin2 that included age, sex, and BMI as covariates.²¹ Sequencing data were filtered to remove ASVs present in <25% of samples and then underwent total sum scaling to generate relative abundances, which were log-transformed prior to model fitting. All P values were adjusted for multiple hypothesis testing by the Benjamini-Hochberg method to generate q -values. Significance was set at $q < .25$ for all analyses, as is recommended for MaAsLin2.²¹ Differential abundance testing for metabolites was performed for normalized,

log-transformed metabolomics data using linear models with empirical Bayes moderation with the limma R package.

Random Forests Classifiers

Fecal microbes, fecal metabolites, and plasma metabolites with $P < .05$ in differential abundance analyses were inputted into the caret R package to generate random forest classifiers with 5-fold cross-validation.²² Contribution of each feature to classifier accuracy was assessed by variable importance scores calculated by caret. Features were retained in the final model if they had an importance score >2 in an initial model iteration. The accuracy of the resulting classifiers was determined by calculating the area under the receiver operating characteristic curve (AUC) with 95% confidence intervals by bootstrapping using the ci.auc function in the pROC R package.

SR Scores and Logistic Regression

Fecal microbe, fecal metabolite, and plasma metabolite random forest classifiers were applied to each sample to generate a probability of belonging to the high SR group. These values ranging from 0 to 1 were used as SR scores and then inputted into logistic regression models (glm function in R, family = “binomial”) to predict clinical flare during longitudinal follow-up; biologic usage, log₁₀ of the fecal calprotectin, and duration of follow-up were included as covariates. Subjects were included in the logistic regression models if they had a minimum of 6 months of longitudinal follow-up or experienced a clinical flare.

Results

Fecal Microbial Signature of High SR

Ninety-one UC patients in clinical and biochemical remission were recruited for cross-sectional assessment and longitudinal follow-up. Remission was defined as Simple Colitis Clinical Activity Index score <5 and fecal calprotectin <150 $\mu\text{g/g}$ at the time of study enrollment; mean SCCAI was 1.1, and mean fecal calprotectin was 22.8 $\mu\text{g/g}$. The patient population consisted of 44% males, with a mean age of 38 years (Supplementary Table 1). The participants showed a range of disease phenotypes by the Montreal classification, with 20% having proctitis (E1), 48% having left-sided disease (E2), and 32% having extensive disease (E3); 70% were taking mesalamine, 16% were taking an immunomodulator (azathioprine, 6-mercaptopurine, or methotrexate), and 31% were taking a biologic (anti-TNF or anti-integrin). Based upon our prior analysis of psychological instruments in this cohort, the 91 participants were divided into those with high or low SR using 2 questionnaires completed at baseline: Perceived Stress Scale and International Personality Item Pool—Neuroticism.⁵ The 91 subjects were assigned to high ($n = 47$) and low ($n = 44$) SR groups using a clustering algorithm (Figure 1A). There were no differences in demographic traits, disease extent, or medication usage between the high and low SR groups (Supplementary Table 1). As anticipated, PSS and IPIP-N significantly differed between the 2 SR groups: 18.3 vs 8.6 and 26.5 vs 15.0, respectively. There was also no difference between the 2 SR groups in fecal calprotectin (23.7 $\mu\text{g/g}$ vs 21.9 $\mu\text{g/g}$), but consistent with our prior observations, the high SR group had significantly higher baseline SCCAI than the low SR group (1.4 vs 0.8).⁵

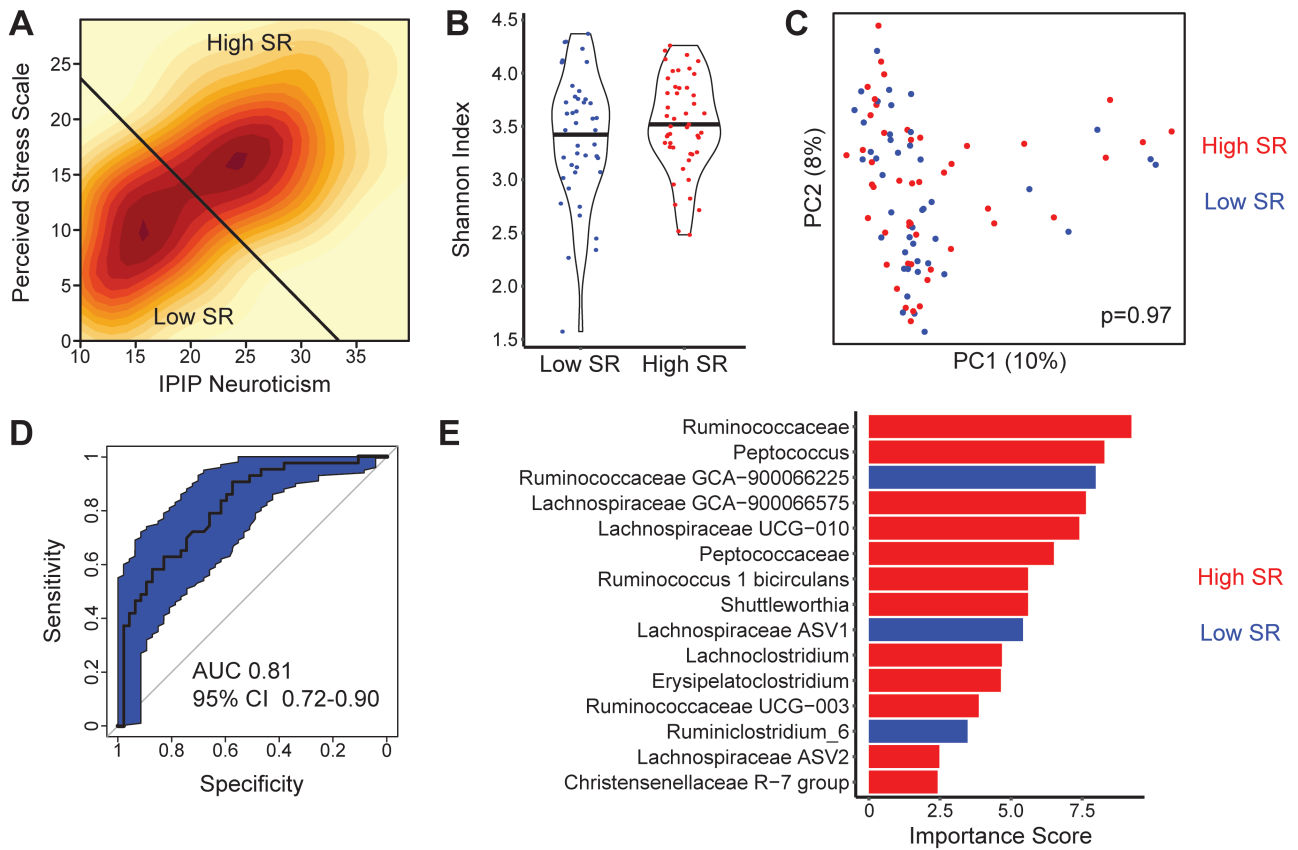


Figure 1. Microbial taxa differentiate ulcerative colitis patients with high vs low SR. A, Density plot for ulcerative colitis patients by International Personality Item Pool—Neuroticism (IPIP-N) and Perceived Stress Scale (PSS). A line divides the patients into high and low SR groups defined by unsupervised clustering. B, Bacterial alpha diversity was assessed by the Shannon Index and visualized by violin plots. C, Principal coordinates analysis (PCoA) plot of Bray-Curtis dissimilarity visualizing bacterial composition across the cohort. Each dot represents one subject, colored by SR group. *P* value for significance of differences between the SR groups was calculated by PERMANOVA. D, Receiver operating characteristics (ROC) curve for a random forest classifier to differentiate high vs low SR. Area under the curve (AUC) for the classifier is shown along with a 95% confidence interval (CI). E, Importance scores of amplicon sequence variants (ASVs) in the random forest classifier, colored by whether the ASVs had higher abundance in the high or low SR group. Taxonomy is shown to the lowest identified taxonomic level, in most cases genus.

Fecal samples collected at baseline underwent 16S rRNA gene sequencing to characterize microbial composition. There was no significant difference in microbial alpha diversity between the 2 SR groups as assessed by the Shannon index, which incorporates both richness and evenness (Figure 1B). Microbial beta diversity, which assesses compositional differences across samples, also did not demonstrate significant differences between the 2 SR groups (Figure 1C). Differential abundance testing of individual bacteria at the level of amplicon sequence variants (ASVs)—roughly corresponding to species—was performed with general linear models adjusting for age, sex, and BMI. None of the nominally significant ASVs retained significance after adjusting for multiple hypothesis testing. We then applied a machine learning strategy to characterize the microbial signature of high SR. A random forest classifier differentiated high vs low SR with high accuracy as measured by area under the receiver operating characteristic curve (AUC) of 0.81 (95% confidence interval [CI] 0.72-0.90; Figure 1D). The classifier consisted of 15 ASVs including multiple members of the Ruminococcaceae (eg, *Ruminococcus bicirculans*), Lachnospiraceae (eg, *Lachnoclostridium*), and Peptococcaceae (eg, *Peptococcus*) families (Figure 1E). Most

microbes in the classifier had higher abundance in the high SR group.

Fecal and Plasma Metabolites Can Differentiate High vs Low SR

We then performed global untargeted metabolomics of feces to assess for microbial functional shifts related to high SR. There was a trend towards a significant global difference in the fecal metabolome between the high and low SR groups ($P = .08$; Figure 2A). General linear models demonstrated that 11 metabolites had significantly different abundance in high SR vs low SR. This included increased levels in the high SR group of anthranilate (a potential product of bacterial tryptophan breakdown) and trans-urocanate, and decreased levels of 4 bile acids (eg, glycocholate, glycochenodeoxycholate, chenodeoxycholic acid sulfate, lithocholic acid sulfate), 4 monoacylglycerols (eg, 1- and 2- linoleoylglycerol and oleoylglycerol), and an acylcarnitine (oleoylcarnitine; Figure 2B). A random forest classifier for SR group based on fecal metabolites had similar accuracy as the fecal microbe classifier, with an AUC of 0.83 (95% CI, 0.75-0.91; Figure 2C). The classifier consisted of 17 metabolites, including 7 of the 11 metabolites that significantly differed between SR groups (Figure 2D). Additional metabolites

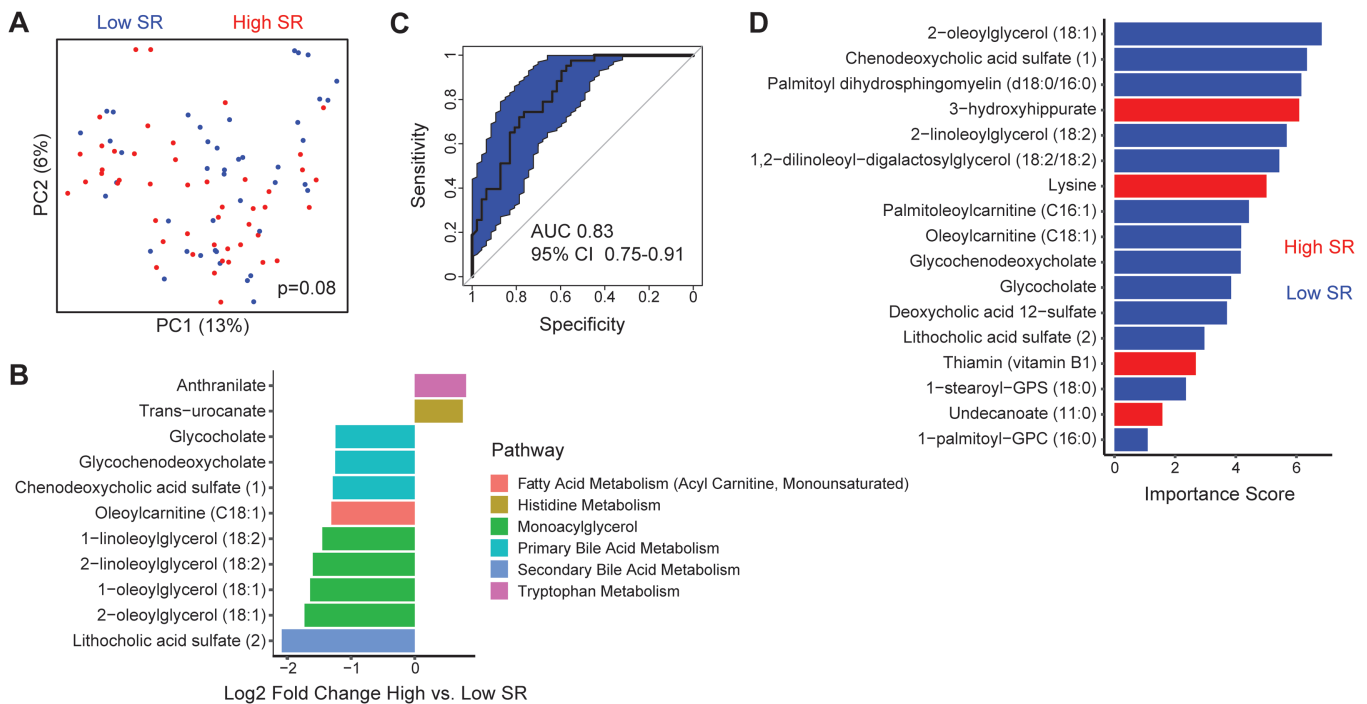


Figure 2. High SR is associated with shifts in the fecal metabolome including reduced levels of monoacylglycerols and bile acids. A, PCoA plot of Euclidean distance visualizing differences in fecal metabolite abundances across subjects, colored by SR group. *P* value determined by PERMANOVA. B, Differentially abundant metabolites between SR groups ($q < .25$) adjusting for age, sex, and BMI. Metabolites are colored by pathway annotation. C, ROC curve of a random forest classifier for high vs low SR based on fecal metabolite abundances. D, Importance scores of fecal metabolites contributing to the random forest classifier, colored by whether the metabolite had higher abundance in high or low SR.

in the classifier included palmitoyl dihydrosphingomyelin, 3-hydroxyhippurate (a microbial product of polyphenol metabolism), lysine, and another bile acid (deoxycholic acid 12-sulfate); decreased in the high SR group).

As some microbial metabolites produced in the intestine can be taken up into the circulation, we then assessed the plasma metabolome for evidence of a microbial metabolite signature of SR. The overall plasma metabolome did not significantly differ between the high and low SR groups (Figure 3A). There were no plasma metabolites that significantly differed by SR group after adjusting for multiple hypothesis testing. However, a random forest classifier generated from plasma metabolites effectively differentiated high vs low SR, with an AUC of 0.91 (95% CI, 0.83-0.96; Figure 3B). Of the 19 metabolites in the classifier, 8 had increased levels in the high SR group including 4-ethylphenyl sulfate (a bacterial metabolite implicated in neurological disorders), sphingomyelin, 7-methylurate (a caffeine metabolite), and N-alpha-acetylornithine (a diet-derived metabolite; Figure 3C).^{23,24} The high SR group had lower levels of 1-arachidonoylglycerol (an endocannabinoid), ribitol (a cell wall component of many Gram-positive bacteria), glutarylcarinitine (an acylcarnitine), steroid hormones (eg, androsterone glucuronide, androstenediol-3 β ,17 β disulfate), amino acid metabolites (eg, argininate, N-acetylasparagine, leucylglycine, N-acetyl-2-aminoadipate), and mannitol/sorbitol (diet-derived sugar alcohols).²⁵

Microbial and Metabolite Measures of SR During Clinical Remission Predict Risk of Clinical Flare

Eighty-nine study participants continued with longitudinal follow-up for at least 6 months (range 6-24 months, mean

14.5 months) or until their first flare. Of these, 31 (35%) experienced a clinical flare. As previously reported, the high SR group had increased frequency of clinical flare compared with the low SR group (45% vs 23%).⁵ We investigated whether microbial and metabolite signatures of SR were similarly predictive of flare risk. To integrate complex data sets into single metrics of SR propensity based upon the microbiome and metabolome, SR scores were calculated from fecal microbiota, fecal metabolites, and plasma metabolites using predicted probabilities from the random forest classifiers. These scores were then incorporated into logistic regression models to evaluate the relationship of these SR metrics to flare risk after adjusting for biologic use, baseline fecal calprotectin, and duration of follow-up. The Fecal Microbiota SR score calculated from 16S rRNA gene sequencing data showed a significant association with clinical flare risk, with an odds ratio of 3.8 for flare (95% CI, 1.0-15.1; Figure 4A). The same approach was then taken for the fecal and plasma metabolomics data. Fecal Metabolite SR score was predictive of clinical flare with odds ratio of 4.1 (95% CI, 1.2-15.2; Figure 4B). Plasma metabolite SR score was also significantly associated with increased flare risk, with the highest odds ratio of the 3 metrics at 4.9 (95% CI, 1.3-19.1; Figure 4C). Baseline fecal calprotectin and duration of follow-up showed increased odds of flare and biologic use showed decreased odds of flare in all 3 regression models, but none of these covariates trended towards significance.

Clinical Flare Is Associated With Shifts in Fecal Metabolites and Attenuation of Metabolite but not Microbial SR Signatures

Fecal microbial composition of participants who flared was assessed longitudinally by 16S rRNA gene sequencing of fecal

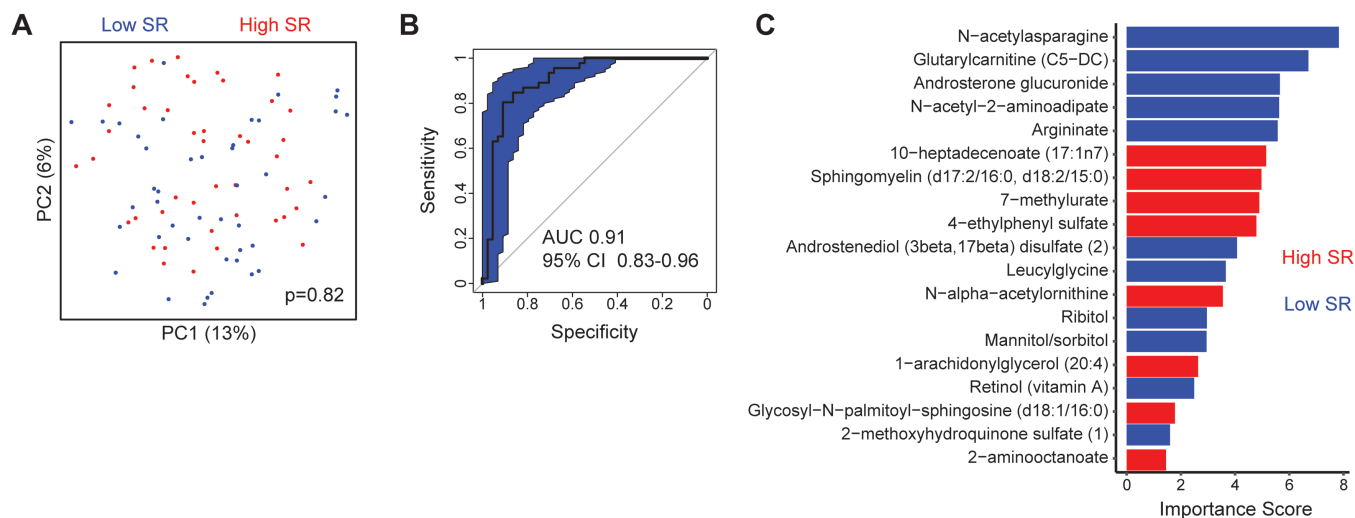


Figure 3. Plasma metabolite signature including increased 4-ethylphenyl sulfate differentiates ulcerative colitis patients with high SR. A, PCoA plot of Euclidean distance visualizing differences in plasma metabolite abundances across subjects, colored by SR group. *P* value determined by PERMANOVA. B, ROC curve of a random forest classifier for high vs low SR constructed from plasma metabolites. C, Importance score of plasma metabolites in the random forest classifier.

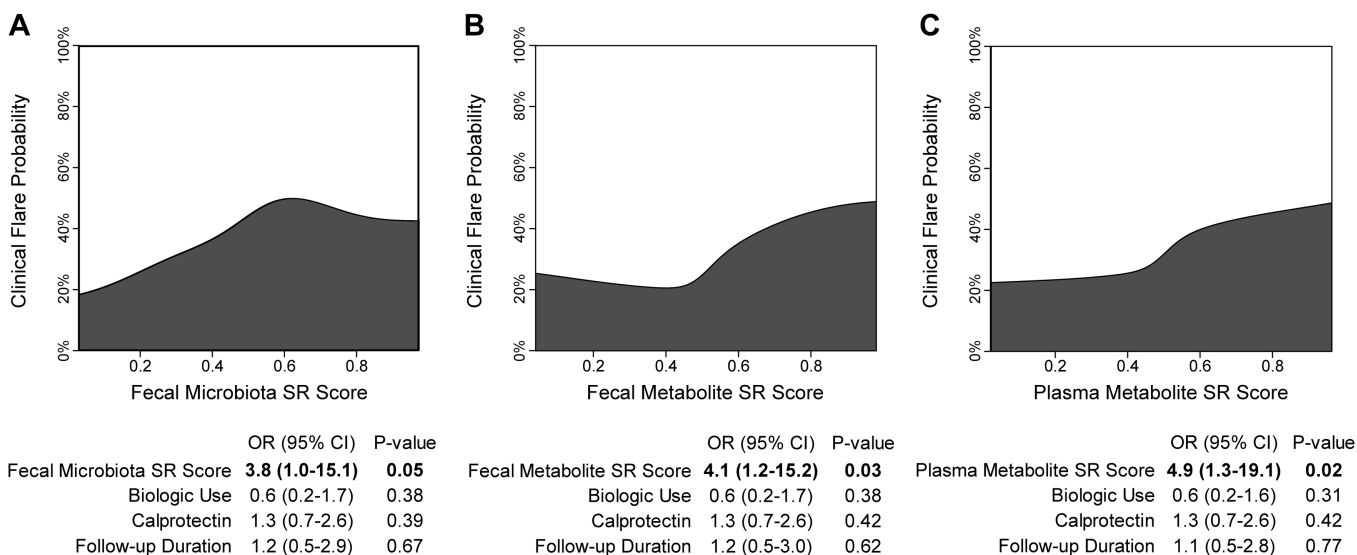


Figure 4. Microbial SR scores derived from microbial composition and fecal and plasma metabolomics are significantly associated with clinical flare risk. Conditional density plots showing clinical flare probability across SR scores (range 0-1) derived from (A) fecal microbiota, (B) fecal metabolites, or (C) plasma metabolites. Logistic regression models were constructed to predict clinical flare from SR scores with biologic use, baseline fecal calprotectin (log transformed), and duration of follow-up (years) as additional predictors. Odds ratio (OR) with 95% confidence interval (CI) is shown for the highest (1) vs lowest (0) SR scores; bold font indicates $P < .05$.

samples collected every 3 months and at the time of flare. There was no significant relationship of microbial alpha or beta diversity with either flare status (comparing flare to all prior nonflare samples) or time to flare (Figure 5A-B). There were also no differentially abundant taxa significantly associated with clinical flares or time to flare. One potential explanation for the lack of microbial association with flare was that only some clinical flares demonstrated evidence of intestinal inflammation by fecal calprotectin. The mean fecal calprotectin at the time of clinical flare was 346 $\mu\text{g/g}$, with only 31% of clinical flares associated with fecal calprotectin >250 $\mu\text{g/g}$ (Supplementary Table 1). However, there were no significant associations of fecal calprotectin with microbial alpha or beta diversity or abundances of individual taxa (Figure 5A-B). We

then assessed whether the SR microbial signature was affected by clinical flare or intestinal inflammation. There was no significant association of fecal microbiota SR score with time to flare, flare status, or fecal calprotectin (Figure 5C).

Longitudinal functional assessment was performed by fecal and plasma metabolomics of samples collected at the time of clinical flare. Fecal metabolite abundances globally showed significant association with both clinical flare ($P = .05$) and with fecal calprotectin ($P = .009$; Figure 6A). We then assessed whether clinical flare and inflammation influenced the metabolite signature of SR, although the fecal metabolite SR score remained significantly higher in high SR subjects than in low SR subjects at the time of flare, the difference was attenuated compared with the difference seen at baseline (Figure

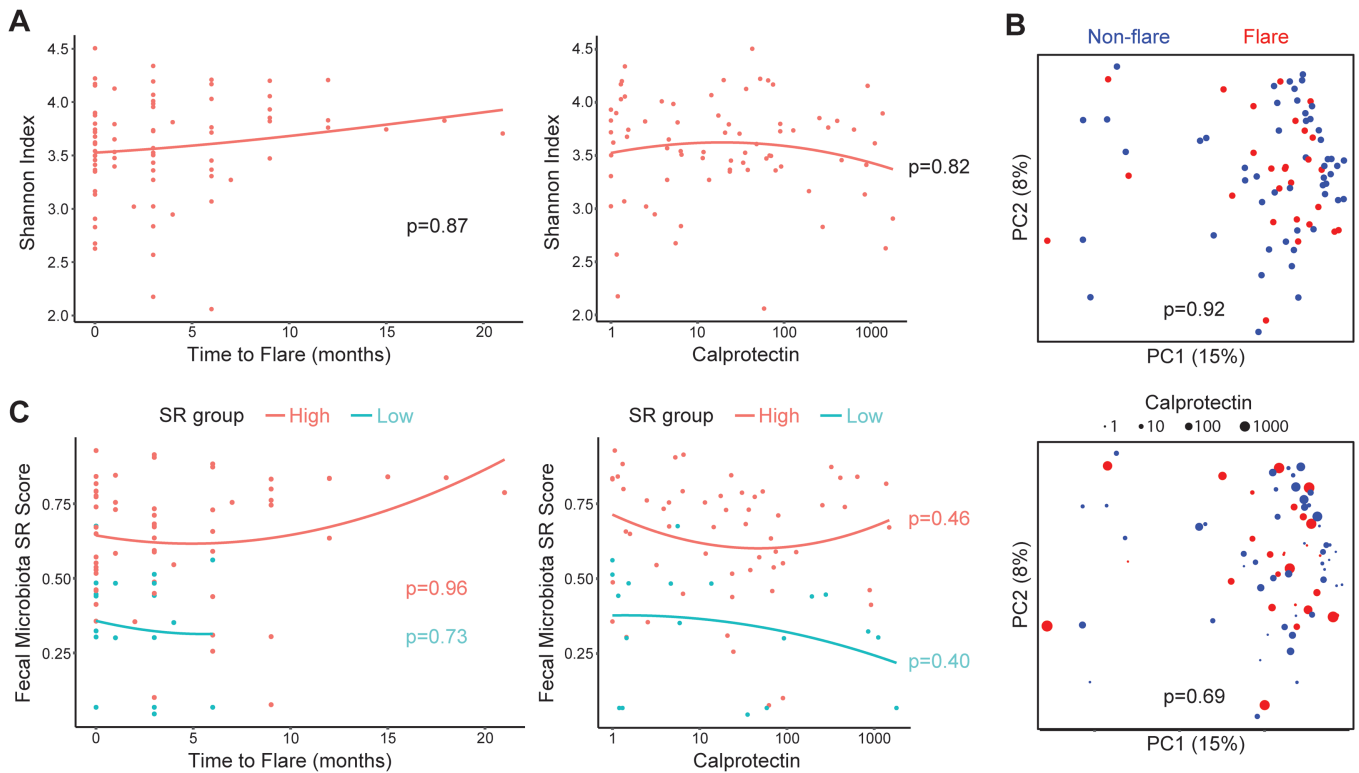


Figure 5. Clinical flares and biochemical inflammation are not associated with shifts in microbial composition or change in microbial SR score. A, Microbial alpha diversity as assessed by the Shannon index is shown for samples collected at quarterly intervals and time of flare from patients who experienced a clinical flare while enrolled in this study. Time points are shown by time to flare (ie, higher times represent earlier timepoints). Loess smoothed curves are shown by SR group. B, PCoA plots showing fecal microbial composition at baseline, quarterly follow-up visits, and time of flare. Each dot represents one sample. Samples taken at the time of flare are shown in red; in the lower panel, dot size is proportional to fecal calprotectin in the sample. *P* values were calculated by repeated measures aware PERMANOVA adjusting for age, sex, BMI, and subject. C, Fecal microbiota SR scores were calculated for longitudinal fecal samples and shown by time to flare and by fecal calprotectin at the time of sampling. *P* values were calculated by linear mixed-effects models adjusting for age, sex, BMI, and subject.

6B). There was a significant association of fecal metabolite SR score with fecal calprotectin levels in each of the 2 SR groups, with higher score in low SR subjects with elevated calprotectin and lower score in high SR subjects with elevated fecal calprotectin (Figure 6C). This suggests that inflammation may dampen the fecal metabolite signature of SR at the time of clinical flare.

Differential metabolite testing demonstrated significant shifts in 23 fecal metabolites between baseline and clinical flare (Figure 6D). There were 29 differential fecal metabolites associated with fecal calprotectin, of which 13 overlapped with those associated with clinical flare (Figure 6E). The overlapping metabolite shifts consisted of increased levels of sphingolipids including sphingomyelin, palmitoyl sphingomyelin, and lactosylceramides (lactosyl-N-nervonoyl-sphingosine, lactosyl-N-palmitoyl-sphingosine, lactosyl-N-stearoyl-sphingosine), lysophospholipids (1-stearoyl-GPE, 1-stearoyl-GPC, 1-stearoyl-GPS), other phospholipids (1,2-dipalmitoyl-GPC, 1-[1-enyl-stearoyl]-GPE, glycerophosphoethanolamine), and linoleoyl-arachidonoyl-glycerol (18:2/20:4). Additional related metabolites were positively associated with just fecal calprotectin including palmitoyl dihydrosphingomyelin, ceramide (sphingomyelin component), glycosyl-N-palmitoyl-sphingosine, 1-palmitoyl-2-oleoyl-GPC, 1-palmitoyl-GPC, 1-stearoyl-2-oleoyl-GPC, 1-(1-enyl-oleoyl)-GPE, and 1-(1-enyl-palmitoyl)-GPE. The only overlapping decreased metabolite was cytidine, a

nucleoside related to cytosine; cytosine was negatively associated with fecal calprotectin.

Plasma metabolomics demonstrated a trend towards differences at the time of clinical flare compared with baseline ($P = .12$) but no association with fecal calprotectin (Figure 7A). Consistent with this, there were no differentially abundant metabolites at the time of clinical flare or associated with fecal calprotectin. Plasma metabolite SR score was assessed at the time of clinical flare and, similar to the Fecal Metabolite SR score, showed an attenuated but still significant difference between high and low SR subjects at the time of flare (Figure 7B). Plasma metabolite SR score in the high SR group decreased with higher calprotectin and in the low SR group increased with higher calprotectin, though these trends did not reach significance ($P = .11$ and $P = .08$, respectively; Figure 7C).

Discussion

Current understanding of the interaction of stress with the microbiome in inflammatory bowel disease (IBD) has been driven by preclinical studies which have consistently found that experimental stressors alter the microbiome.⁶ Human studies have demonstrated microbiome associations in IBD with comorbid depression and/or anxiety; however, little is known about the relationship of the microbiome with IBD patients' stress perception and response.⁶ Here, we report that SR in UC in clinical remission is characterized by a

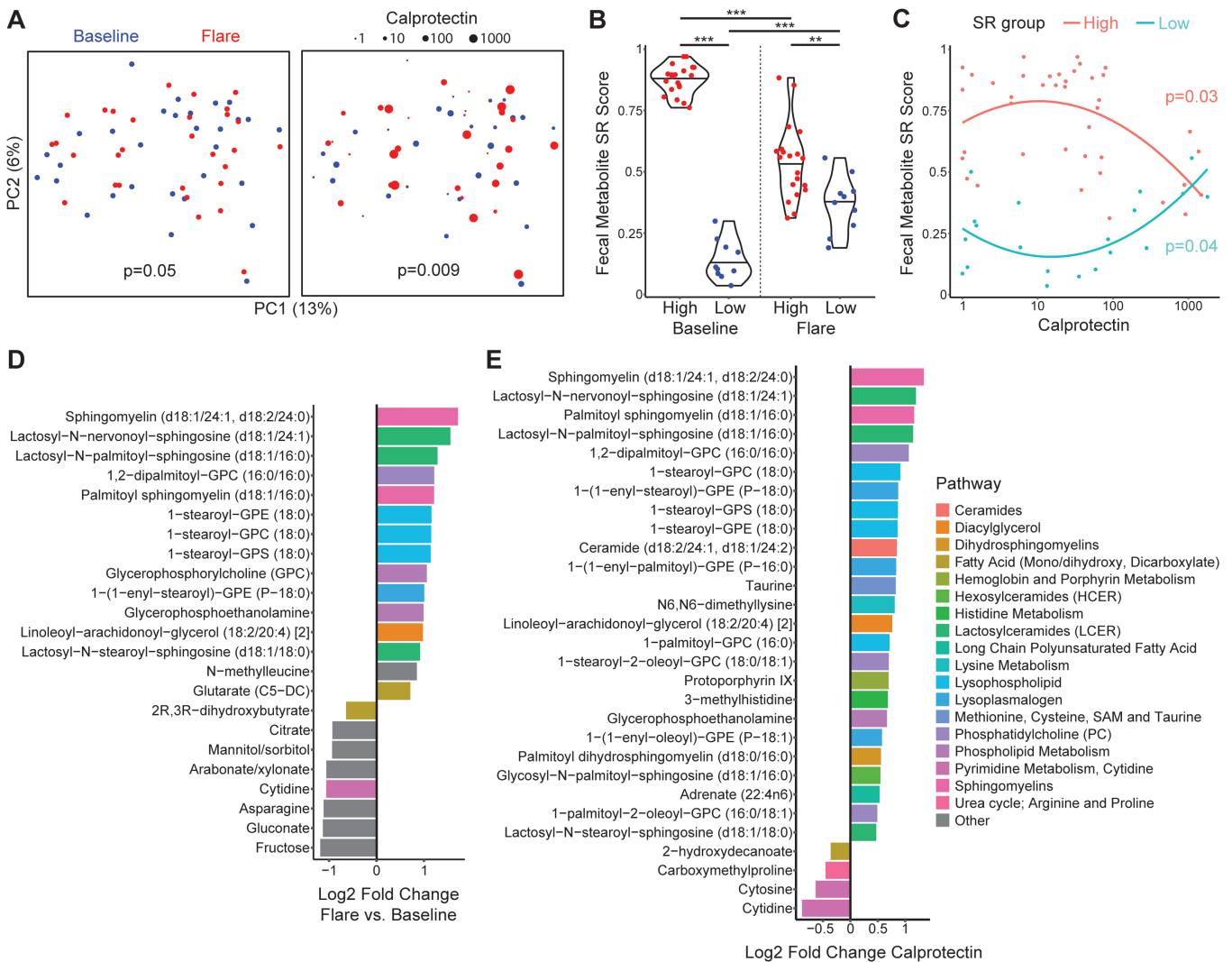


Figure 6. Fecal metabolites are associated with clinical flares and biochemical inflammation. **A**, PCoA plots showing fecal metabolite profiles at baseline and time of flare from subjects who experienced a clinical flare. Each dot represents one sample. Samples taken at the time of flare are shown in red; in the right panel, dot size is proportional to fecal calprotectin in the sample. *P* values were calculated by repeated measures ANOVA PERMANOVA adjusting for age, sex, BMI, and subject. **B**, Fecal metabolite SR scores are shown for fecal samples collected at baseline and at the time of flare, stratified by SR group. $***P < .01$, $**P < .001$. **C**, Fecal metabolite SR scores from samples taken at baseline or time of flare are shown by fecal calprotectin at the time of sampling. *P* values were calculated by linear mixed-effects models adjusting for age, sex, BMI, and subject. **D**, Differentially abundant metabolites between the time of flare and baseline adjusting for age, sex, BMI, and subject. **E**, Differentially abundant metabolites associated with fecal calprotectin adjusting for flare vs baseline status, age, sex, BMI, and subject. Log₂-fold change for difference of 1 in log₁₀ calprotectin (eg, 10 vs 100, 100 vs 1000) is shown. Metabolites are colored by pathway annotation.

microbial compositional signature that remains consistent during clinical remission and disease flare. Ten out of 15 microbes contained within the fecal microbiota SR score were members of the Ruminococcaceae and Lachnospiraceae families. Interestingly, 2 large microbiome association studies of 2594 and 3211 subjects reported that 10 out of 12 microbial genera and 15 out of 23 ASVs that were associated with depression belonged to the Ruminococcaceae and Lachnospiraceae families.^{26,27} This supports that microbes contained within these 2 bacterial families are involved in brain-gut-microbiome pathways. Stress reactivity was not associated with global alterations of microbial diversity and community structure in our study. In contrast, a prior study of UC and Crohn’s disease patients in clinical remission had reported that high values on a perceived stress questionnaire (PSQ, a distinct instrument from PSS

in this study) was associated with lower microbial diversity by the Shannon index and significant differences in beta diversity.²⁸ The 6 taxa that were associated with PSQ group in that study did not overlap with the microbes included in the fecal microbiota SR score. The distinct findings in these 2 studies may reflect differences in study population (UC vs all IBD, exclusion of subjects in clinical remission with elevated calprotectin in our study, American vs Swiss subjects), sample type (feces vs intestinal biopsies), adjustment for covariates, and definition of stress groups.

The association of microbial profiles with SR could arise from a bidirectional interaction in which effector arms of stress responses including the HPA axis and ANS influence the gut microbiome, which in turn signals to the brain to modulate stress response. Stress-induced shifts in the microbiome in animal models have been shown to promote intestinal

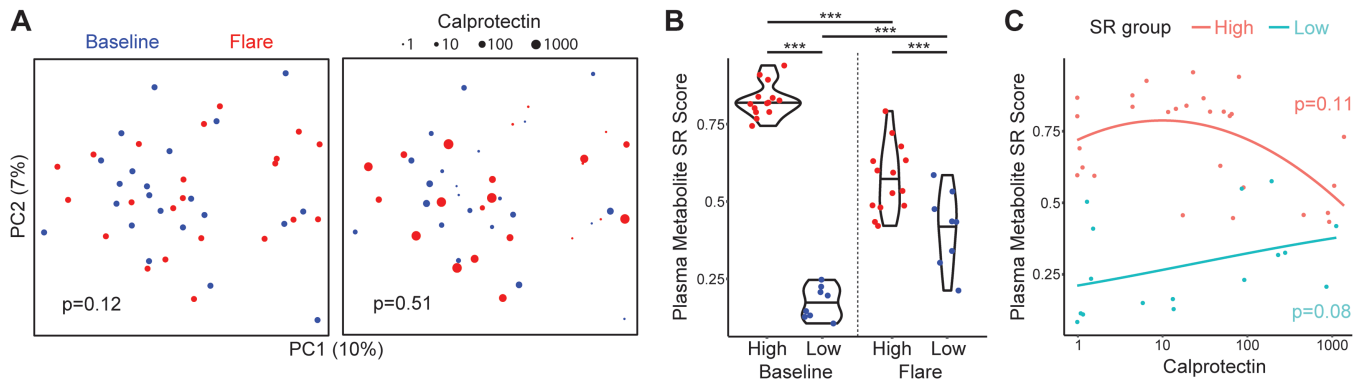


Figure 7. Attenuation of the plasma metabolite SR signature at the time of clinical flare. A, PCoA plots showing plasma metabolite profiles at baseline and time of flare. Samples taken at the time of flare are shown in red; in the right panel, dot size is proportional to fecal calprotectin. *P* values were calculated by repeated measures aware PERMANOVA adjusting for age, sex, BMI, and subject. B, Plasma metabolite SR scores are shown for samples collected at baseline and at the time of flare, stratified by SR group. ****P* < .001 (C) Plasma metabolite SR scores from samples taken at baseline or time of flare are shown by fecal calprotectin at the time of sampling. *P* values were calculated by linear mixed-effects models adjusting for age, sex, BMI, and subject.

inflammation, hyperglycemia, and neuroinflammation; these phenotypes are transferrable to other animals via the microbiome and prevented by antibiotic treatment.^{29,30} It is unclear whether stress-induced alteration of microbial composition and function could influence SR, but this possibility is supported by preclinical studies demonstrating that the absence of a microbiome results in an exaggerated HPA response to stress and that probiotics can alter aspects of stress response.^{31,32} Signaling from SR-associated gut microbes to the brain could occur through the production of microbial neuroactive metabolites in the intestine that travel through the circulation to the brain.³³

In support of a potential effect of neuroactive bacterial metabolites on central stress response in high SR patients, fecal and plasma metabolomics demonstrated SR-associated metabolites that have the potential to impact the brain. Among these were several metabolites in the endocannabinoid system. The high SR group showed significantly decreased fecal levels of 4 monoacylglycerols, including 2-linoleoylglycerol and 2-oleoylglycerol, which are congeners of the endocannabinoid 2-arachidonoylglycerol (2-AG).³⁴ The high SR group also showed reduced plasma levels of 1-arachidonoylglycerol (1-AG), an endocannabinoid with CB1 agonist activity, though less than 2-AG.²⁵ These results parallel the findings of a mouse model of unpredictable chronic stress, in which stress-exposed mice had reduced serum levels of monoacylglycerols including 2-linoleoylglycerol, 2-oleoylglycerol, and 1-AG.³⁵ Moreover, depressive-like behaviors and reduced serum monoacylglycerols could be transferred via the microbiome of stress-exposed mice, indicating that the microbiota after chronic stress mediates alteration of the endocannabinoid system. The depressive-like behaviors induced by microbiome transfer were reversed by pharmacologically increasing endocannabinoid signaling. Ulcerative colitis subjects with high SR may have a similar microbiome-mediated alteration of the endocannabinoid system affecting central stress response.

The high SR group also had reduced fecal levels of primary bile acids (eg, chenodeoxycholic acid sulfate, glycocholate, glycochenodeoxycholate) and secondary bile acids (eg, lithocholic acid sulfate, deoxycholic acid 12-sulfate). Although bile acids have been extensively studied for their effects on

intestinal and hepatic function, there has also been interest in their neurological effects. The brain has bile acid levels similar to those seen in circulation and expresses multiple bile acid receptors.³⁶ Preclinical studies have demonstrated that bile acid receptor agonists can ameliorate models of neurodegenerative and neuroinflammatory diseases including Parkinson's disease, Alzheimer's disease, amyotrophic lateral sclerosis, and multiple sclerosis.³⁶ In a mouse model of chronic stress, overexpression of the bile acid receptor FXR resulted in exacerbated depression-like behavior, whereas reduction in FXR expression by short hairpin RNA reduced the behavioral phenotype.³⁷ These findings support that the altered bile acid levels observed in the high SR group could influence stress-related outcomes in the brain, though this may reflect downstream consequences of altered intestinal bile acid receptor signaling, as significant differences in bile acids were only seen in feces and not in plasma.

The plasma metabolomics signature of high SR included increased levels of a metabolite, 4-EPS, previously reported to affect experimental models of neurodevelopmental and affective disorders.^{23,24} In particular, it has been demonstrated that 4-EPS can enter the brain and reduce myelination of neuronal axons, which alters brain activity patterns and promotes anxiety-like behavior in a mouse model.²⁴ It is conceivable that increased 4-EPS emanating from the gut microbiome in UC patients could increase SR by altering neuronal signaling in regions of the brain involved in stress responses.

The observed dampening of SR fecal and plasma metabolite signatures in both high and low SR groups with elevated fecal calprotectin suggests that the metabolite changes of SR are distinct from those of active intestinal inflammation. Further supporting this, there was little overlap between the fecal metabolite signatures of high SR and clinical flare or intestinal inflammation. Clinical flare and intestinal inflammation measured by fecal calprotectin were both characterized by increased fecal levels of many sphingolipids and other phospholipids, which is consistent with a prior metabolomics study reporting elevated fecal sphingolipids in UC.³⁸ Among the sphingolipids, sphingomyelin was notable, as it previously has been demonstrated to promote colitis in animal models, possibly by enhancing intestinal epithelial injury.³⁹

In summary, we found that UC patients in clinical and biochemical remission can be accurately stratified into high and low SR groups by microbial and metabolite profiles and that these signatures predict clinical flare risk. Limitations of this study include the lack of endoscopic assessment of disease activity, use of 16S rRNA gene sequencing (which does not consistently achieve species resolution) for microbiome composition assessment, and sample size. Although the number of subjects was greater than that in some prior IBD studies of microbial biomarkers for clinical flare risk, individual microbe and plasma metabolite associations with high SR fell short of significance after adjusting for covariates and correcting *P* values for the large number of features being measured.⁴⁰ Nevertheless, robust signatures could be derived by integrating multiple microbes and metabolites. These findings may have clinical implications for the development of biomarkers to identify high SR individuals who are prone to clinical flares and would benefit from stress-directed interventions. This study also highlighted candidate microbes and microbial metabolites for further study as mediators of microbiome-gut-brain signaling in stress-induced UC flares.

Supplementary Data

Supplementary data are available at *Inflammatory Bowel Diseases* online.

Acknowledgments

Authors would like to thank Jean Stains and Cathy Liu for their assistance with study coordination and data management, respectively, and the Microbiome Core of the Goodman-Luskin Microbiome Center for its support with sequencing.

Author Contribution

Study concept and design—J.P.J., J.S.S., E.A.M.; acquisition of data—A.I.A., F.L., W.K., H.J.R., A.K., V.L., J.L., B.N.; analysis and interpretation of data—J.P.J.; drafting of the manuscript—J.P.J.; critical revision of the manuscript—all authors; obtained funding—J.P.J., J.S.S., E.A.M.; study supervision—J.P.J., J.S.S., E.A.M.

Funding

This research was supported by the Crohn's and Colitis Foundation Environmental Triggers Research Initiatives grant #56313 (J.P.J., J.S.S., E.A.M.) and National Institutes of Health R01 DK048351 (E.A.M.). J.P.J. was supported by VA CDA2 IK2CX001717.

Conflicts of Interest

E.A.M.: scientific advisory board member of Danone, Axial Biotherapeutics, Amare, Mahana Therapeutics, Pendulum, Bloom Biosciences, Seed, Salvo, APC Microbiome Ireland. J.S.S.: CorEvitas—Consulting; Abbvie—Speaker's Bureau; Prometheus—Advisory Board. No other authors have anything to disclose.

Data Availability

The 16S rRNA sequencing data generated for this study are available through the NCBI BioProject, PRJNA951422. The

fecal and plasma metabolomics data are available as [supplementary data](#) files.

References

1. Singh S, Graff LA, Bernstein CN. Do NSAIDs, antibiotics, infections, or stress trigger flares in IBD? *Am J Gastroenterol*. 2009;104(5):1298-1313; quiz 1314.
2. Bernstein CN, Singh S, Graff LA, et al. A prospective population-based study of triggers of symptomatic flares in IBD. *Off J Am Coll Gastroenterol | ACG*. 2010;105(9):1994-2002.
3. Langhorst J, Hofstetter A, Wolfe F, Häuser W. Short-term stress, but not mucosal healing nor depression was predictive for the risk of relapse in patients with ulcerative colitis: a prospective 12-month follow-up study. *Inflamm Bowel Dis*. 2013;19(11):2380-2386.
4. Levenstein S, Prantera C, Varvo V, et al. Stress and exacerbation in ulcerative colitis: a prospective study of patients enrolled in remission. *Am J Gastroenterol*. 2000;95(5):1213-1220.
5. Sauk JS, Ryu HJ, Labus JS, et al. High Perceived stress is associated with increased risk of ulcerative colitis clinical flares. *Clin Gastroenterol Hepatol*. 2023;21(3):741-749.e3.
6. Ge L, Liu S, Li S, et al. Psychological stress in inflammatory bowel disease: psychoneuroimmunological insights into bidirectional gut-brain communications. *Front Immunol*. 2022;13:1016578.
7. Bonaz BL, Bernstein CN. Brain-gut interactions in inflammatory bowel disease. *Gastroenterology*. 2013;144(1):36-49.
8. Moussaoui N, Jacobs JP, Larauche M, et al. Chronic early-life stress in rat pups alters basal corticosterone, intestinal permeability, and fecal microbiota at weaning: influence of sex. *J Neurogastroenterol Motil*. 2017;23(1):135-143.
9. Lee M, Chang EB. Inflammatory bowel diseases (IBD) and the microbiome—searching the crime scene for clues. *Gastroenterology*. 2021;160(2):524-537.
10. Rhee SH, Pothoulakis C, Mayer EA. Principles and clinical implications of the brain–gut–enteric microbiota axis. *Nat Rev Gastroenterol Hepatol*. 2009;6(5):306-314.
11. Labanski A, Langhorst J, Engler H, Elsenbruch S. Stress and the brain-gut axis in functional and chronic-inflammatory gastrointestinal diseases: a transdisciplinary challenge. *Psychoneuroendocrinology*. 2020;111:104501.
12. Marin IA, Goertz JE, Ren T, et al. Microbiota alteration is associated with the development of stress-induced despair behavior. *Sci Rep*. 2017;7(1):43859.
13. Walmsley RS, Ayres RCS, Pounder RE, Allan RN. A simple clinical colitis activity index. *Gut*. 1998;43(1):29-32.
14. Bewtra M, Brensinger CM, Tomov VT, et al. An optimized patient-reported ulcerative colitis disease activity measure derived from the Mayo score and the simple clinical colitis activity index. *Inflamm Bowel Dis*. 2014;20(6):1070-1078.
15. Tong M, Jacobs JP, McHardy IH, Braun J. Sampling of intestinal microbiota and targeted amplification of bacterial 16S rRNA genes for microbial ecologic analysis. *Curr Protoc Immunol*. 2014;107(1):7 41 41-47 41 11.
16. Jacobs JP, Goudarzi M, Singh N, et al. A Disease-associated microbial and metabolomics state in relatives of pediatric inflammatory bowel disease patients. *Cell Mol Gastroenterol Hepatol*. 2016;2(6):750-766.
17. Callahan BJ, McMurdie PJ, Rosen MJ, et al. DADA2: High-resolution sample inference from illumina amplicon data. *Nat Methods*. 2016;13(7):581-583.
18. Jacobs JP, Lagishetty V, Hauer MC, et al. Multi-omics profiles of the intestinal microbiome in irritable bowel syndrome and its bowel habit subtypes. *Microbiome*. 2023;11(1):5.
19. McMurdie PJ, Holmes S. phyloseq: an R package for reproducible interactive analysis and graphics of microbiome census data. *PLoS One*. 2013;8(4):e61217.
20. Anderson MJ. A new method for non-parametric multivariate analysis of variance. *Austral Ecol*. 2001;26(1):32-46.

21. Mallick H, Rahnavard A, McIver LJ, et al. Multivariable association discovery in population-scale meta-omics studies. *PLoS Comput Biol.* 2021;17(11):e1009442.
22. Breiman L. Random forests. *Mach Learn.* 2001;45(1):5-32.
23. Hsiao EY, McBride SW, Hsien S, et al. Microbiota modulate behavioral and physiological abnormalities associated with neurodevelopmental disorders. *Cell.* 2013;155(7):1451-1463.
24. Needham BD, Funabashi M, Adame MD, et al. A gut-derived metabolite alters brain activity and anxiety behaviour in mice. *Nature.* 2022;602(7898):647-653.
25. Farah SI, Hilston S, Tran N, Zvonok N, Makriyannis A. 1-, 2- and 3-AG as substrates of the endocannabinoid enzymes and endogenous ligands of the cannabinoid receptor 1. *Biochem Biophys Res Commun.* 2022;591:31-36.
26. Radjabzadeh D, Bosch JA, Uitterlinden AG, et al. Gut microbiome-wide association study of depressive symptoms. *Nat Commun.* 2022;13(1):7128.
27. Bosch JA, Nieuwdorp M, Zwinderman AH, et al. The gut microbiota and depressive symptoms across ethnic groups. *Nat Commun.* 2022;13(1):7129.
28. Humbel F, Rieder JH, Franc Y, et al.; Swiss IBD Cohort Study Group. Association of alterations in intestinal microbiota with impaired psychological function in patients with inflammatory bowel diseases in remission. *Clin Gastroenterol Hepatol.* 2020;18(9):2019-2029.e11.
29. Delaroque C, Chervy M, Gewirtz AT, Chassaing B. Social overcrowding impacts gut microbiota, promoting stress, inflammation, and dysglycemia. *Gut Microbes.* 2021;13(1):2000275.
30. Jagers RM, DiSabato DJ, Loman BR, et al. Stressor-induced reduction in cognitive behavior is associated with impaired colonic mucus layer integrity and is dependent upon the LPS-binding protein receptor CD14. *J Inflamm Res.* 2022;15:1617-1635.
31. Sudo N, Chida Y, Aiba Y, et al. Postnatal microbial colonization programs the hypothalamic-pituitary-adrenal system for stress response in mice. *J Physiol.* 2004;558(Pt 1):263-275.
32. Bear T, Dalziel J, Coad J, et al. The microbiome-gut-brain axis and resilience to developing anxiety or depression under stress. *Microorganisms.* 2021;9(4):723.
33. Martin CR, Osadchiy V, Kalani A, Mayer EA. The brain-gut-microbiome axis. *Cell Mol Gastroenterol Hepatol.* 2018;6(2):133-148.
34. Sihag J, Di Marzo V. (Wh)olistic (E)ndocannabinoidome-microbiome-axis modulation through (N)utrition (WHEN) to curb obesity and related disorders. *Lipids Health Dis.* 2022;21(1):9.
35. Chevalier G, Siopi E, Guenin-Mace L, et al. Effect of gut microbiota on depressive-like behaviors in mice is mediated by the endocannabinoid system. *Nat Commun.* 2020;11(1):6363.
36. Hurley MJ, Bates R, Macnaughtan J, Schapira AHV. Bile acids and neurological disease. *Pharmacol Ther.* 2022;240:108311.
37. Hu W, Wu J, Ye T, et al. Farnesoid X receptor-mediated cytoplasmic translocation of CRTCL2 disrupts CREB-BDNF signaling in hippocampal CA1 and leads to the development of depression-like behaviors in mice. *Int J Neuropsychopharmacol.* 2020;23(10):673-686.
38. Franzosa EA, Sirota-Madi A, Avila-Pacheco J, et al. Gut microbiome structure and metabolic activity in inflammatory bowel disease. *Nat Microbiol.* 2019;4(2):293-305.
39. Fischbeck A, Leucht K, Frey-Wagner I, et al. Sphingomyelin induces cathepsin D-mediated apoptosis in intestinal epithelial cells and increases inflammation in DSS colitis. *Gut.* 2011;60(1):55-65.
40. Braun T, Di Segni A, BenShoshan M, et al. Individualized dynamics in the gut microbiota precede Crohn's disease flares. *Am J Gastroenterol.* 2019;114(7):1142-1151.